Support material for

Mechanistic Insights into Chloroacetic Acid Production from Atmospheric Multiphase VOC-Chlorine Chemistry

Mingxue Li[1], Men Xia[2,3], Chunshui Lin[1], Yifan Jiang[1], Weihang Sun[1], Yurun Wang[1], Yingnan Zhang[1], Maoxia He[4], Tao Wang*[,1]

[1]Department of Civil and Environmental Engineering, The Hong Kong Polytechnic University, Hong Kong 999077, China

[2]Institute for Atmospheric and Earth System Research/Physics, Faculty of Science, University of Helsinki, Helsinki 00014, Finland

[3]Aerosol and Haze Laboratory, Beijing Advanced Innovation Center for Soft Matter Science and Engineering, Beijing University of Chemical, Beijing 100029, China

[4]Environment Research Institute, Shandong University, Qingdao 266237, China

Correspondence: Tao Wang (tao.wang@polyu.edu.hk)

This document includes Supplementary Tables S1-S4, and Supplementary Figures S1-S11.

Table of contents

Table S1. Identified Cl-OVOCs and their precursors in previous VOC-Cl chamber experiments.

Cl-OVOCs	structure	precursor	structure	Ref.
formyl chloride		isoprene	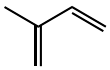	1,2
		methyl vinyl ketone	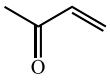	2
		methacrolein	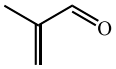	2
		1,3-butadiene	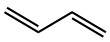	2
		1-butene	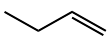	2
		methyl acrylate	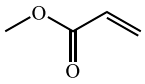	3
		methyl 3-chloro-2-oxopropanoate	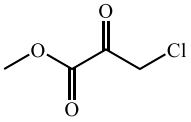	1
chloro-acetaldehyde	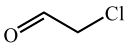	1-butene	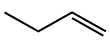	2
		acrolein	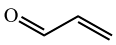	4
		methyl vinyl ketone	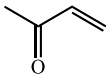	2,4
		allyl alcohol	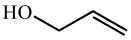	5
		3-buten-2-ol	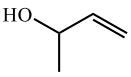	5
		2-methyl-3-buten-2-ol	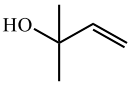	5
chloroacetone	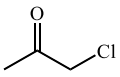	methacrolein	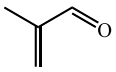	2,4,6
		2-methyl-2-propen-1-ol	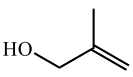	5
		3-methyl-3-buten2-one	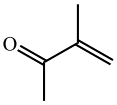	7

methyl 3-chloro-2-oxopropanoate	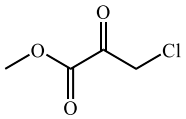	methyl acrylate	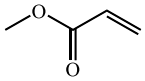	3
3-choloro-4-hydroxy-2-butanone	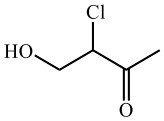	crotyl alcohol	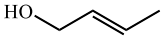	5
2-chloro-propanal	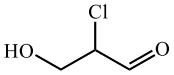	crotyl alcohol	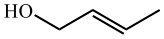	5
4-chloro-crotonaldehyde	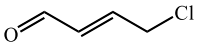	1,3-butadiene	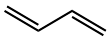	2,8
chloro-methyl vinyl ketone	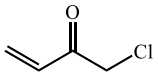	1,3-butadiene	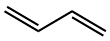	8
		isoprene	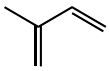	1
chloro-methylbutenal	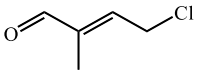	isoprene	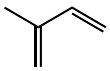	1
chloro-methylbutenone	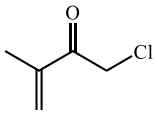	isoprene	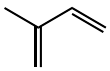	1,2

Table S2. Input data of the chemical box model for the campaign-averaged conditions.

Parameter	Diurnal average[a]	Parameter	Diurnal average
T (K)	297.0 ± 1.0	propane (ppb)	1.0 ± 0.2
RH (%)	74.7 ± 5.0	isobutane (ppb)	0.39 ± 0.07
SO_2 (ppb)	2.7 ± 0.1	n-butane (ppb)	0.6 ± 0.1
CO (ppb)	264.8 ± 10.4	isopentane (ppb)	0.35 ± 0.07
NO (ppb)	0.33 ±0.24	n-pentane (ppb)	0.23 ± 0.03
NO_2 (ppb)	3.2 ± 0.7	2-methylpentane (ppb)	0.36 ± 0.08
N_2O_5 (ppb)	0.036 ± 0.029	n-hexane (ppb)	0.16 ± 0.05
HONO (ppb)	0.15 ± 0.03	cyclohexane (ppb)	0.022 ± 0.001
O_3 (ppb)	49.8 ± 9.9	acetylene (ppb)	1.3 ± 0.2
Sa (um^2 cm^{-3})	181.5 ± 23.2	ethene (ppb)	0.6 ± 0.1
$ClNO_2$ (ppb)	0.29 ± 0.23	propene (ppb)	0.10 ± 0.03
Cl_2 (ppb)	0.016 ± 0.014	isoprene (ppb)	0.17 ± 0.10
HOCl (ppb)	0.039 ± 0.019	α-pinene (ppb)	0.019 ± 0.007
BrCl (ppt)	0.64 ± 0.38	β-pinene (ppb)	0.010 ± 0.004
Br_2 (ppt)	3.1 ± 1.0	toluene (ppb)	0.36 ± 0.06
jNO_2 (10^{-3} s-1)	6.3[b]	benzene (ppb)	0.15 ± 0.02
methane	2000[c]	ethylbenzene (ppb)	0.05 ± 0.01
ethane (ppb)	1.7 ± 0.1	o-xylene (ppb)	0.04 ± 0.02

[a]Daily average ± standard deviation; [b]maximum value; [c]constant value.

Table S3. Branching ratios (Γ) and rate constants (k, 10^{-10} cm^3/molecule s) of alkene + $Cl^{\bullet}$ reactions.

VOC	*updated model*			*original model*	
	Γ	k	Reference	Γ	k
C_3H_6	α-C addition: 92% abstraction: 8%	2.93	[9]	α-C addition: 40% β-C addition: 50% abstraction: 10%	2.70
C_5H_8	α-C addition: 85% abstraction: 15%	4.75	[1]	addition: 100%	4.75
MVK	α-C addition: 75% abstraction: 25%	2.20	[2]	-	2.20
MACR	α-C addition: 86% abstraction: 14%	2.30	[10]	-	1.70

Table S4. QC-calculated energies of solvation and aqueous-phase reactions of OVOCs and their reactive uptake coefficients[1].

OVOC	ΔG_{sol}	$\Delta G^{‡}_{hyd}$	$\Delta_r G_{hyd}$	$\Delta G'_{sol}$	λ	Ref.
formaldehyde	-1.30	41.84	0.17	-8.87	2.00×10^{-3}	[11]
glyoxal	-2.68	41.73	0.35	-11.13	2.90×10^{-3}	[12]
methylglyoxal	-3.30	42.75	1.80	-11.58	3.70×10^{-4}	[13]
2-butanone	-3.43	46.30	7.47	-7.62	1.50×10^{-4}	[14]
acetone	-3.55	47.84	7.93	-11.06	1.80×10^{-4}	[14]
2,3-butanedione	-3.78	45.74	5.41	-8.10	8.00×10^{-5}	[14]
formyl chloride	-1.14	28.79	-7.58	-9.04	2.34×10^{-2}	this work
chloro-acetaldehyde	-3.42	42.31	1.87	-10.92	8.23×10^{-4}	this work
chloro-acetone	-6.52	46.37	8.81	-8.40	7.07×10^{-5}	this work
cholro-butanedione	-4.27	39.58	1.85	-8.55	8.31×10^{-4}	this work
CMBO	-5.16	49.06	10.69	-10.13	3.63×10^{-5}	this work
CAA	-	-	-	-	7.05×10^{-5}	[15]

[1] ΔG_{sol} is solvation energy of OVOC, $\Delta G^{‡}_{hyd}$ and $\Delta_r G_{hyd}$ are the Gibbs free energy barriers and changes in the hydration reactions of OVOC in the aqueous phase, $\Delta G'_{sol}$ is the evaporation energy of diol, λ is the reactive uptake coefficient from references and calculated in this work.

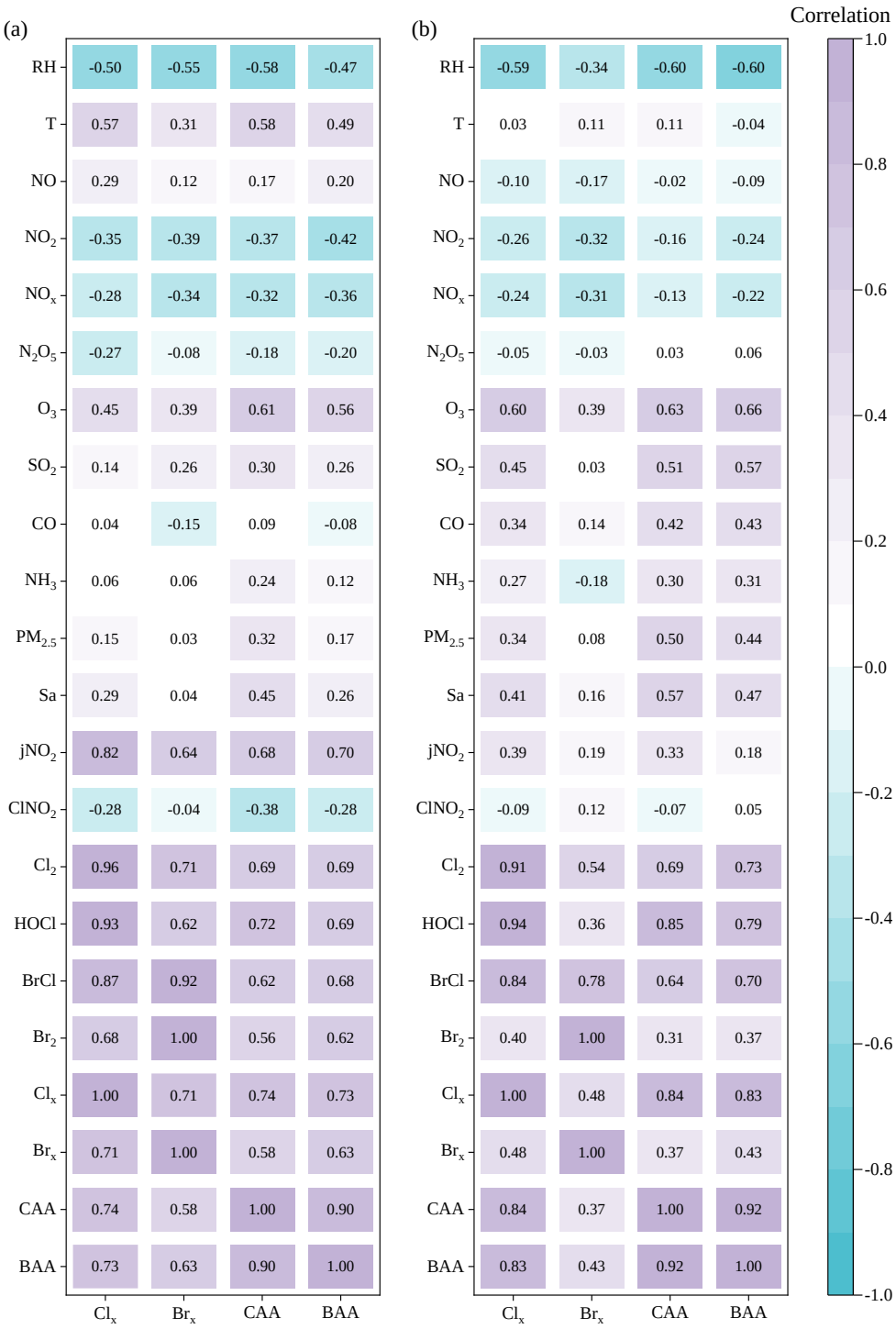

Figure S1. The correlation coefficients between important meteorological factors and CAA concentration in (a) 2020 and (b) 2021. $Cl_x = 2 \times Cl_2 + HOCl + BrCl$, and $Br_x = 2 \times Br_2 + BrCl$. All data are 1-h averages.

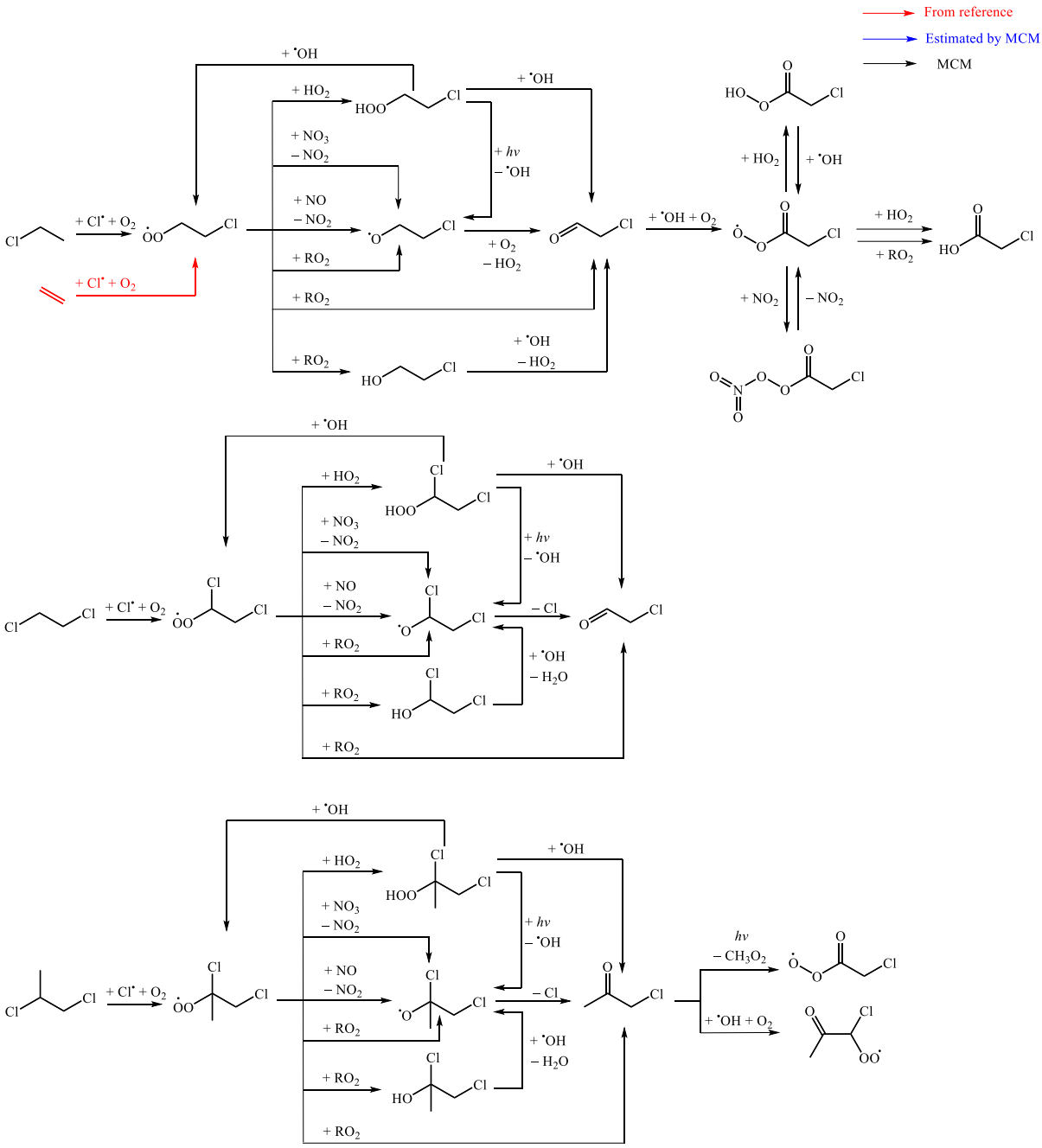

Figure S2. The primary reaction mechanisms of Cl• with 1-chloroethane (C_2H_5Cl), 1,2-dichloroethane ($C_2H_4Cl_2$), 1,2-dichloropropane ($C_3H_6Cl_2$), and ethene (C_2H_4).

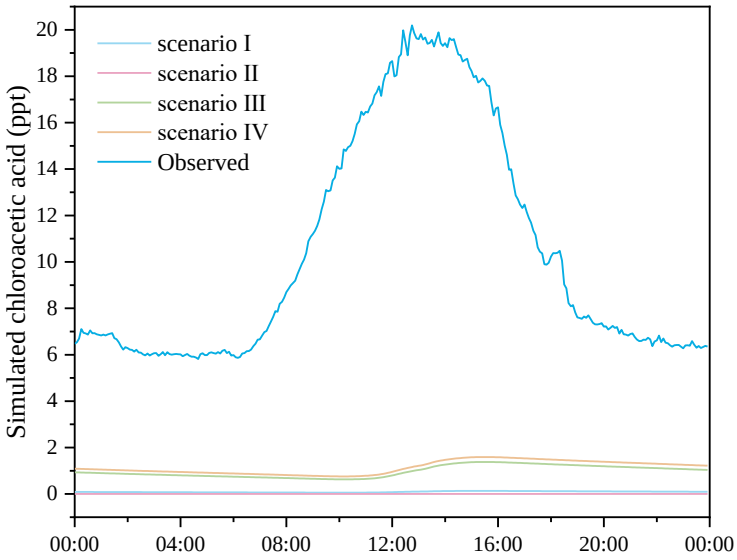

Figure S3. Box model-simulated diurnal profiles of chloroacetic acid in different scenarios. The simulated result of scenario II is close to zero.

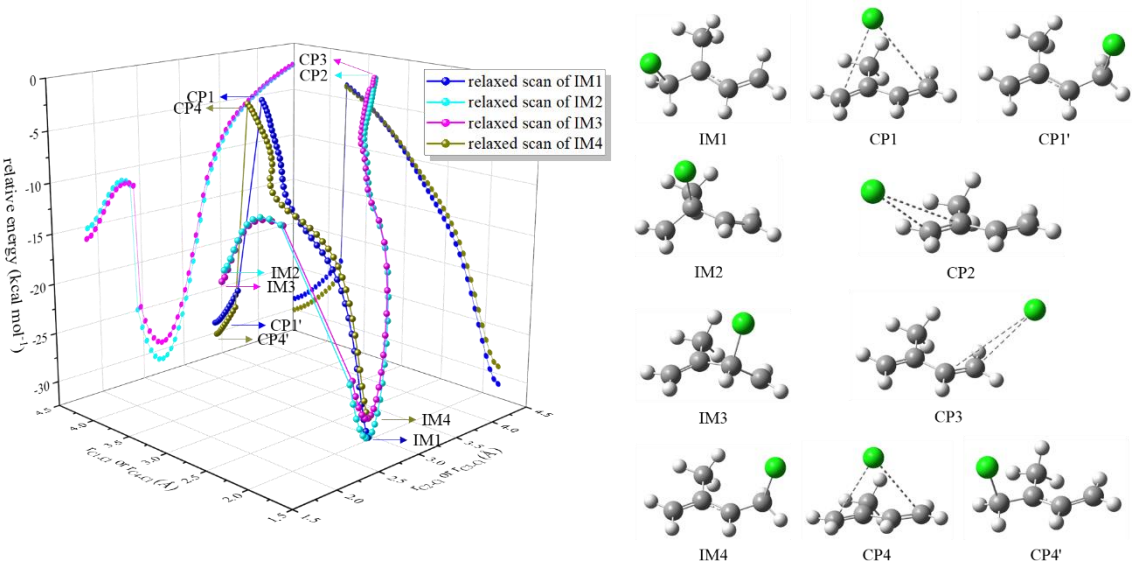

Figure S4. Relaxed scan of Cl• addition to isoprene. IM1, IM2, IM3, and IM4 are intermediates for Cl• addition to 1-, 2-, 3-, and 4-positions of isoprene, and CP1 – CP4, CP1' and CP4' are derived from scans of IM1 – IM2 in terms of bond lengths (r) of C-Cl as variables, respectively. Scanned potential energy surfaces of IM1 – IM4 take the total energy of the reactants Cl• + isoprene as zero for reference. The relative energies of IM1 and IM4 are lowest. A relaxed scan of IM1 reveals a minimum energy path (MEP): CP1' ← CP1 ← IM1, where CP1' approximates IM4. The relaxed scan of IM4 also reveals interconversion between IM1 and IM4, but the energy barriers are too high to be difficult to occur. The relaxed scans of IM2 and IM3 reveal the MEP of IM2 ← IM1 ← CP2 and IM3 ← IM4 ← CP3. Saddle points of IM2 and IM3 are

difficult to reach due to their conversion to IM1 and IM4 passing through low-energy barriers. Thus, Cl˙ prefers to add to 1- and 4-positions of isoprene.

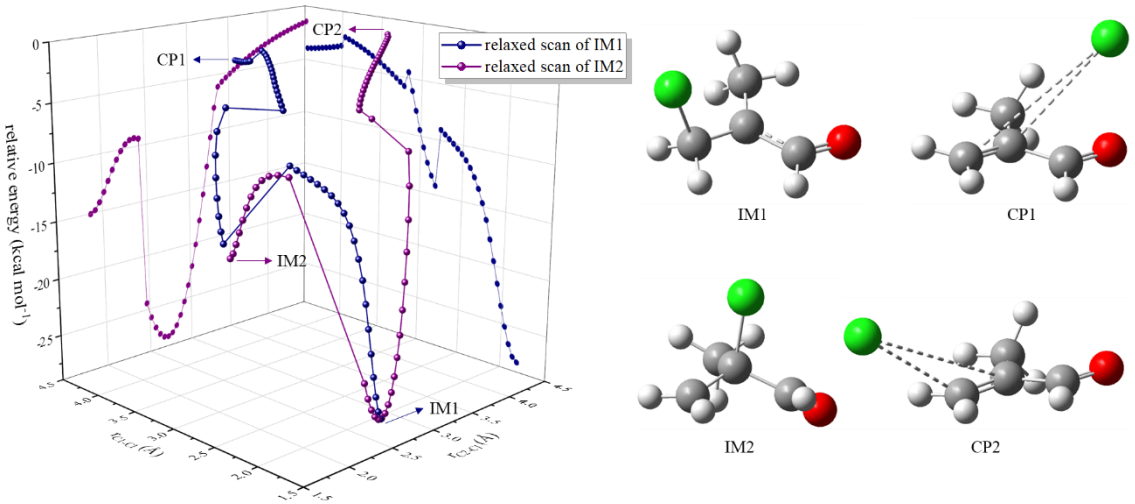

Figure S5. Relaxed scan of Cl˙ addition to methacrolein (MACR). Similar to the Cl˙ addition of propene.

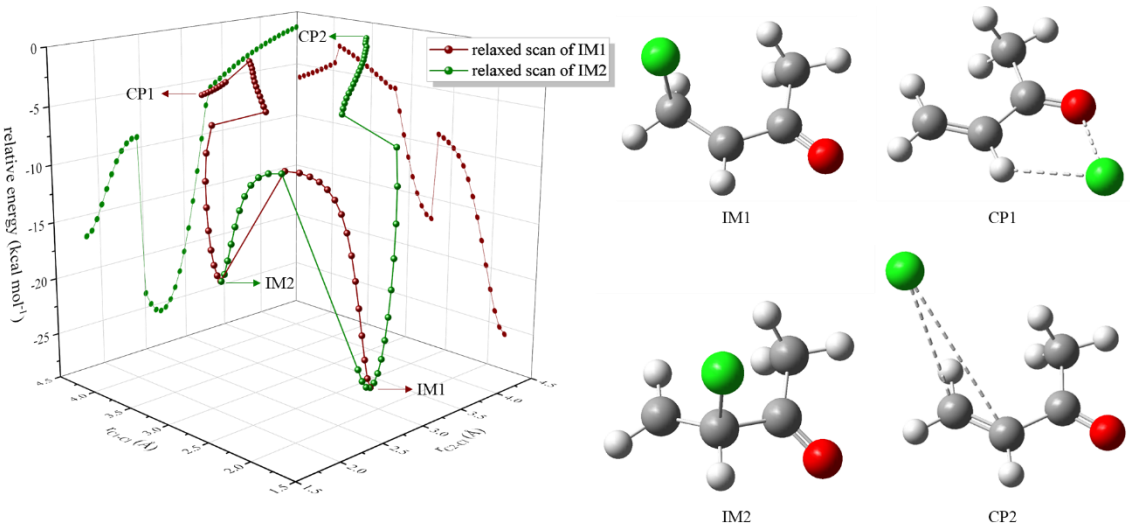

Figure S6. Relaxed scan of Cl˙ addition to methyl vinyl ketone (MVK). Similar to the Cl˙ addition of propene.

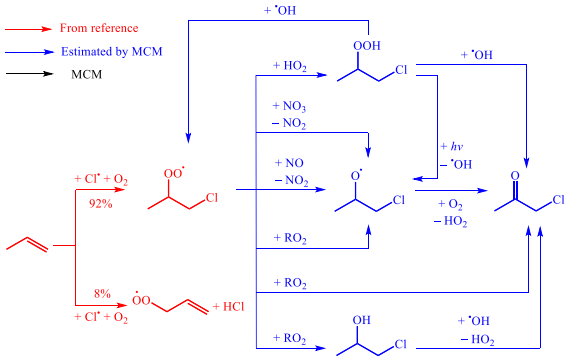

Figure S7. Proposed the primary reaction mechanisms of Cl˙ with propene (C_3H_6).

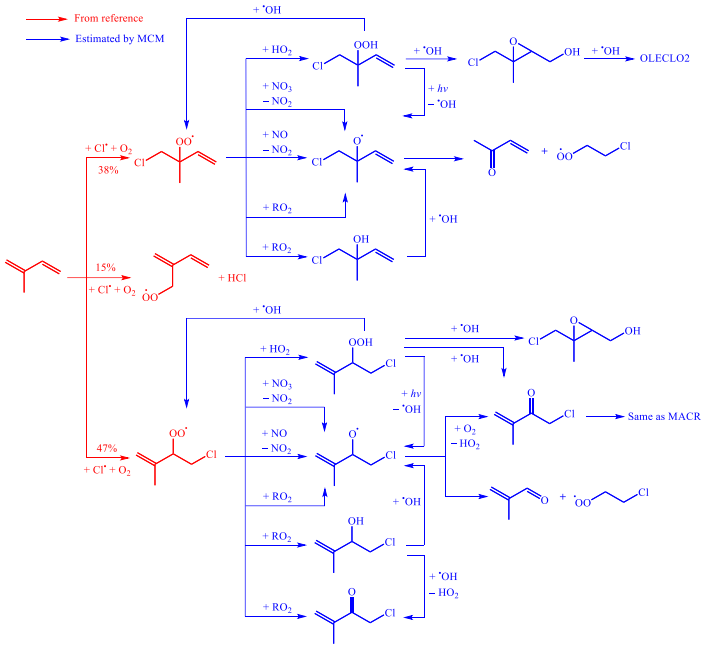

Figure S8. Proposed the primary reaction mechanisms of Cl• with isoprene (C_5H_8).

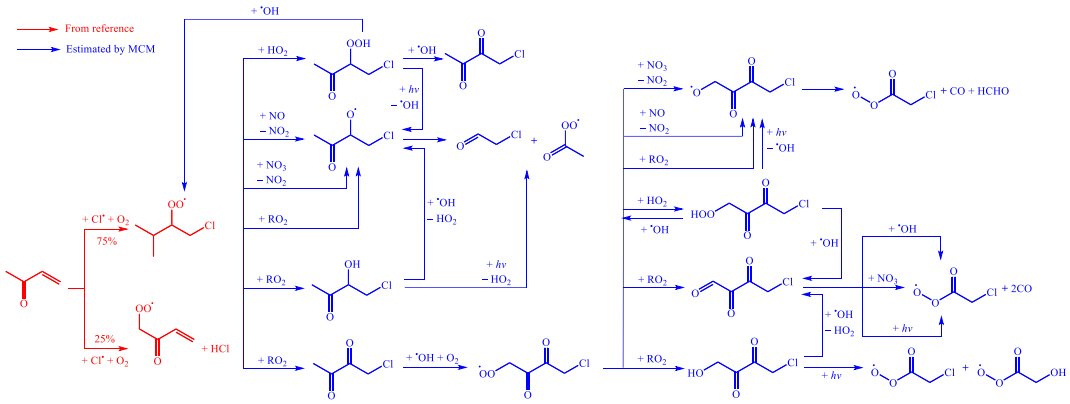

Figure S9. Proposed the primary reaction mechanisms of Cl• with methyl vinyl ketone (MVK).

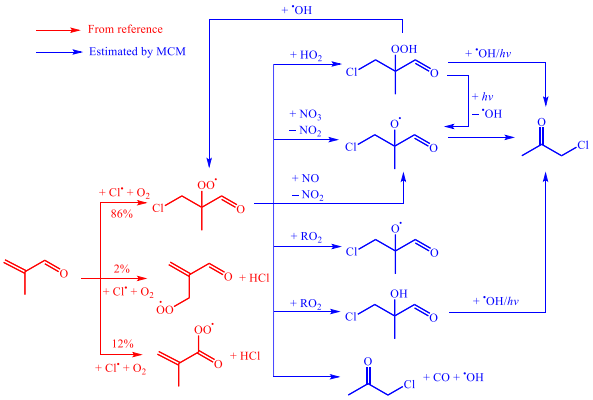

Figure S10. Proposed the primary reaction mechanisms of Cl• with methacrolein (MACR).

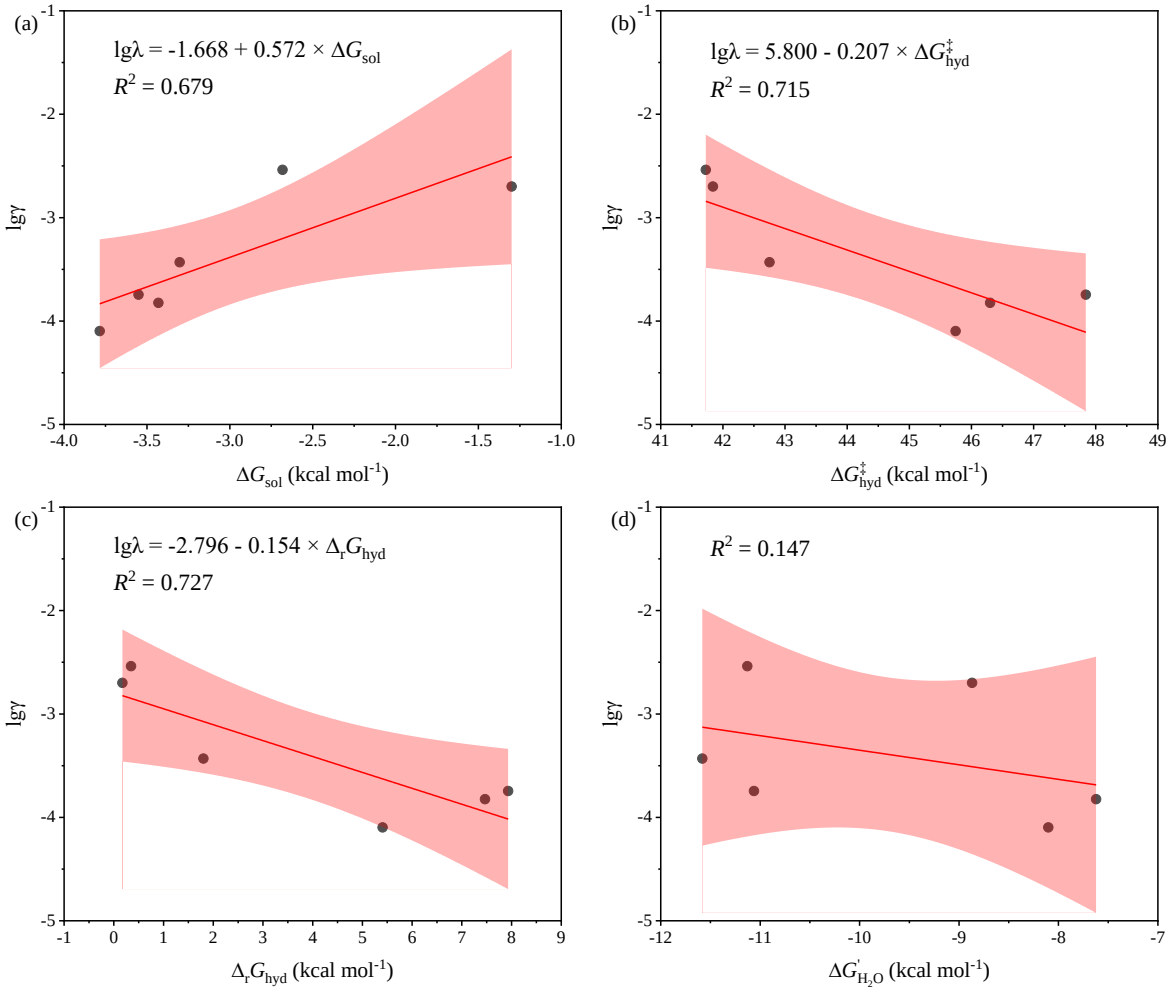

Figure S11. Linear relationships between Gibbs free energy of diol reactions and reactive uptake coefficients of carbonyls. (a) ΔG_{sol} as the solvation energy of carbonyls; (b) $\Delta G^{\ddagger}_{hyd}$ and (c) $\Delta_r G_{hyd}$ as the Gibbs free energy barriers and changes in the hydration reactions of carbonyls; (d) $\Delta G'_{sol}$ as the evaporation energy of diols; λ as the reactive uptake coefficients.

Reference

(1) Wennberg, P. O.; Bates, K. H.; Crounse, J. D.; Dodson, L. G.; McVay, R. C.; Mertens, L. A.; Nguyen, T. B.; Praske, E.; Schwantes, R. H.; Smarte, M. D.; St Clair, J. M.; Teng, A. P.; Zhang, X.; Seinfeld, J. H. Gas-Phase Reactions of Isoprene and Its Major Oxidation Products. *Chem. Rev.* **2018**, *118* (7), 3337–3390. https://doi.org/10.1021/acs.chemrev.7b00439.

(2) Orlando, J. J.; Tyndall, G. S.; Apel, E. C.; Riemer, D. D.; Paulson, S. E. Rate Coefficients and Mechanisms of the Reaction of Cl-Atoms with a Series of Unsaturated Hydrocarbons under Atmospheric Conditions. *Int. J. Chem. Kinet.* **2003**, *35* (8), 334–353. https://doi.org/10.1002/kin.10135.

(3) Blanco, M. B.; Bejan, I.; Barnes, I.; Wiesen, P.; Teruel, M. A. FTIR Product Distribution Study of the Cl and OH Initiated Degradation of Methyl Acrylate at Atmospheric Pressure. *Environ. Sci. Technol.* **2010**, *44* (18), 7031–7036. https://doi.org/10.1021/es101831r.

(4) Canosa-Mas, C. E.; Cotter, E. S. N.; Duffy, J.; Thompson, K. C.; Wayne, R. P. The Reactions of Atomic Chlorine with Acrolein, Methacrolein and Methyl Vinyl Ketone. *Phys. Chem. Chem. Phys.* **2001**, *3* (15), 3075–3084. https://doi.org/10.1039/b101434j.

(5) Rodríguez, A.; Rodríguez, D.; Soto, A.; Bravo, I.; Diaz-de-Mera, Y.; Notario, A.; Aranda, A. Products and Mechanism of the Reaction of Cl Atoms with Unsaturated Alcohols. *Atmos. Environ.* **2012**, *50*, 214–224. https://doi.org/10.1016/j.atmosenv.2011.12.030.
(6) Kaiser, E. W.; Pala, I. R.; Wallington, T. J. Kinetics and Mechanism of the Reaction of Methacrolein with Chlorine Atoms in 1−950 Torr of N_2 or N_2/O_2 Diluent at 297 K. *J. Phys. Chem. A* **2010**, *114* (25), 6850–6860. https://doi.org/10.1021/jp103317c.
(7) Wang, J.; Zhou, L.; Wang, W.; Ge, M. Gas-Phase Reaction of Two Unsaturated Ketones with Atomic Cl and O_3: Kinetics and Products. *Phys. Chem. Chem. Phys.* **2015**, *17* (18), 12000–12012. https://doi.org/10.1039/C4CP05461J.
(8) Wang, W.; Finlayson-Pitts, B. J. Unique Markers of Chlorine Atom Chemistry in Coastal Urban Areas: The Reaction with 1,3-butadiene in Air at Room Temperature. *J. Geophys. Res.* **2001**, *106* (D5), 4939–4958. https://doi.org/10.1029/2000JD900683.
(9) Kaiser, E. W.; Wallington, T. J. Pressure Dependence of the Reaction Cl + C_3H_6. *J. Phys. Chem.* **1996**, *100* (23), 9788–9793. https://doi.org/10.1021/jp960406r.
(10) Sun, C.; Xu, B.; Zhang, S. Atmospheric Reaction of Cl + Methacrolein: A Theoretical Study on the Mechanism, and Pressure- and Temperature-Dependent Rate Constants. *J. Phys. Chem. A* **2014**, *118* (20), 3541–3551. https://doi.org/10.1021/jp500993k.
(11) Iraci, L. T.; Tolbert, M. A. Heterogeneous Interaction of Formaldehyde with Cold Sulfuric Acid: Implications for the Upper Troposphere and Lower Stratosphere. *J. Geophys. Res.* **1997**, *102* (D13), 16099–16107. https://doi.org/10.1029/97JD01259.
(12) Liggio, J.; Li, S.; McLaren, R. Reactive Uptake of Glyoxal by Particulate Matter. *J. Geophys. Res.* **2005**, *110* (D10), 2004JD005113. https://doi.org/10.1029/2004JD005113.
(13) De Haan, D. O.; Jimenez, N. G.; De Loera, A.; Cazaunau, M.; Gratien, A.; Pangui, E.; Doussin, J.-F. Methylglyoxal Uptake Coefficients on Aqueous Aerosol Surfaces. *J. Phys. Chem. A* **2018**, *122* (21), 4854–4860. https://doi.org/10.1021/acs.jpca.8b00533.
(14) Schütze, M.; Herrmann, H. Uptake of Acetone, 2-Butanone, 2,3-Butanedione and 2-Oxopropanal on a Water Surface. *Phys. Chem. Chem. Phys.* **2004**, *6* (5), 965–971. https://doi.org/10.1039/B313474A.
(15) Wang, Y.; Zhou, L.; Wang, W.; Ge, M. Heterogeneous Uptake of Formic Acid and Acetic Acid on Mineral Dust and Coal Fly Ash. *ACS Earth Space Chem.* **2020**, *4* (2), 202–210. https://doi.org/10.1021/acsearthspacechem.9b00263.